Interactions of Polymer Model Surfaces with Cold Plasmas: Hexatriacontane as a Model Molecule of High-Density Polyethylene and Octadecyl Octadecanoate as a Model of Polyester. I. Degradation Rate versus Time and Power

F. CLOUET* and M. K. SHI

Institut Charles Sadron (CRM-EAHP), 6 rue Boussingault, 67083 Strasbourg-Cedex, France

SYNOPSIS

To gain a better understanding of the evolution of polymer surfaces under cold plasmas, model polymer surfaces were studied. The degradation products and the gas phase were investigated by mass and optical emission spectrometry. Their evolution versus time and power enable us to propose a mechanism that involves atomic oxygen, OH• and H• radicals.

INTRODUCTION

Low-temperature plasmas have been widely used to improve polymer surface properties[1-7] by introducing new functional groups.[8-17] These treatments lead to the formation of radicals[18,19] that are, very likely, the promoters of surface crosslinking,[20-23] functionalization, and degradation.[24-27] The modification is the result of different plasma species such as ions, excited neutrals, as well as UV radiation. Therefore, it is very difficult to establish a relationship between these species and the relevant mechanisms. Moreover, polymer surfaces are very often poorly defined because of the presence of initiators and different additives: It can thus be difficult to pinpoint the origin of the modification observed. In order to simplify these systems, we decided to study model polymer surfaces.[28,29] Our goal is to establish a relationship between the physical and the chemical makeup of a polymer and its behavior in cold plasmas. Our strategy is based on the understanding of the surface modification of a very simple model whose chemical structure and morphology are well defined and that of the same model after its endowment with a chemical function. Hexatriacontane ($C_{36}H_{74}$), which is known to share many structural features with high-density polyethylene, has often been chosen as a model of this polymer. Crystallization of this pure C_{36} paraffin is well known and the morphology of its surface was described.[30,31] $C_{36}H_{74}$ crystals are rhombic platelets, the acute angle of lozenge being about 72°. The chains are arranged perpendicularly to the crystal surface, the methyl groups being exactly at the top and the bottom. This model was then modified; one of the central methylene groups of $C_{36}H_{74}$ was replaced by an ester function. The molecule obtained, octadecyl octadecanoate (OOD), crystallizes also in lozenge-shaped tablets as shown in Figure 1. In a first step, we have determined the effect of the presence of an ester function by comparing the behavior of $C_{36}H_{74}$ and OOD under plasma. In a second step, the model molecules have been compared with their corresponding polymers, that is, high-density polyethylene (cristallinity > 90%) and polycaprolactone $-[(CH_2)_5CO_2]_n-$ (cristallinity $\simeq$ 55%), respectively, in order to exemplify the role of the molecular weight of the amorphous domains and the chain ends. This will be the purpose of our next paper.

The cold plasma treatment leads to bond breaking on the polymer surface; the fragments formed are kicked out into the gas phase and can be analyzed by mass spectrometry and optical emission spectroscopy. In this study, we report the influence of the plasma parameters (time, power) investigated in terms of (a) weight loss both on the parafinic model and on the ester, (b) concentration of the small molecules in the effluents originating from surface degradation, and (c) emission intensities of the excited species.

* To whom correspondence should be addressed.

Journal of Applied Polymer Science, Vol. 46, 1955–1966 (1992)
 CCC 0021-8995/92/111955-12

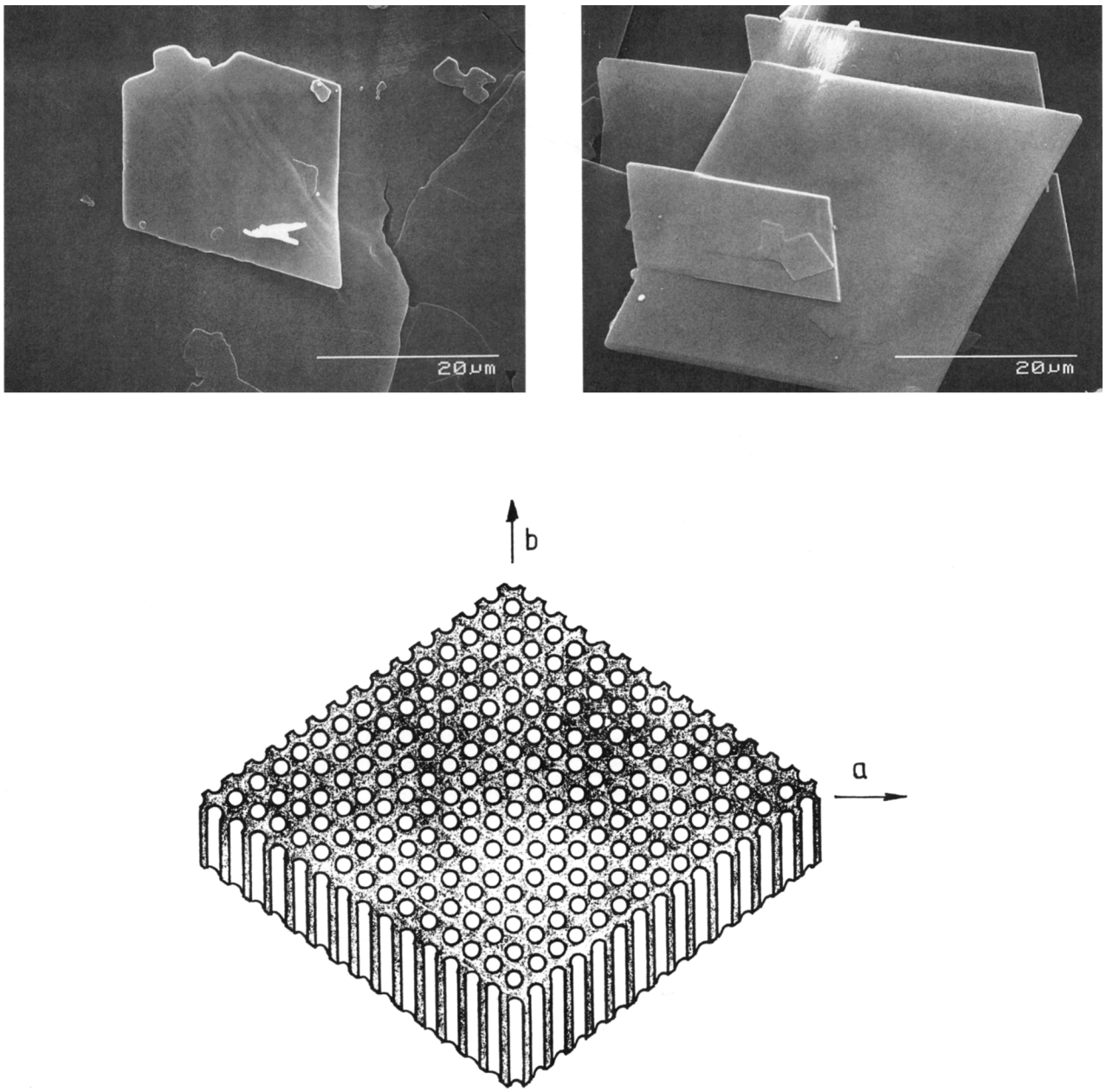

Figure 1 Scanning electron microscopy of $C_{36}H_{74}$ and OOD surfaces prepared by solution slow evaporation.

EXPERIMENTAL

Materials and Apparatus

The solvents were distilled twice under argon on sodium wire. $C_{36}H_{74}$, (98% pure) purchased from Aldrich, was recrystallized from hexane solution. OOD was synthesized by reacting octadecanol at 90°C with octadecanoyl chloride in $CHCl_3$ in the presence of triethylamine as HCl trap. The ester was purified by chromatography on a silica gel column and recrystallized from acetone.

$C_{36}H_{74}$ and OOD films were prepared by slow evaporation under an argon partial vacuum from a benzene or acetone solution, respectively. The solution concentrations were adjusted according to the desired thickness of the films. After their preparation the films were kept under argon.

The stainless-steel reaction vessel (Fig. 2) is a cylinder 15 cm in height and 23 cm in diameter. The

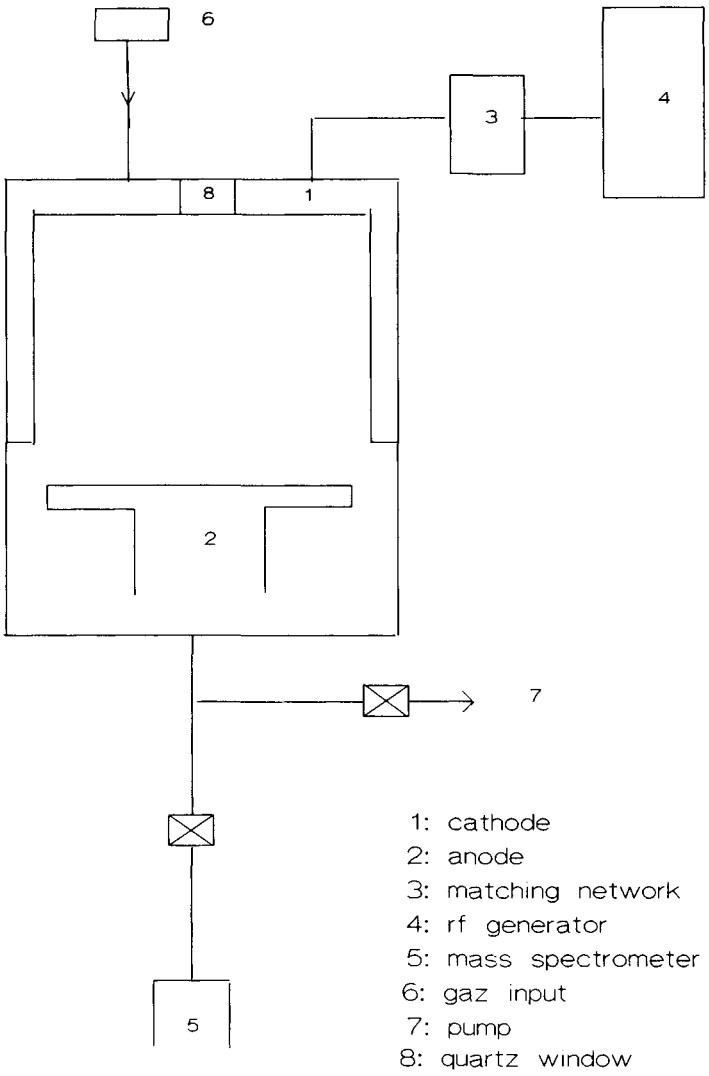

Figure 2 Schematic representation of glow discharge reactor.

lid (1) forms the cathode and the bottom (2), a 15-cm diameter disk, forms the grounded electrode. The power to sustain plasma is supplied by a 13.56-MHz generator (ENI HF 300), which is capacitively coupled to the cathode via an impedance matching network. The substrates rest on the grounded electrode, which is kept at constant temperature by a water circulation. The system is evacuated with a mechanical pump (Alcatel 2033) to 10^{-2} torr vacuum, and the pressure is measured with a Baratron pressure transducer. The gas flow is fed into the reactor through a mass flow meter (unit instrument Fullerton). The evolution of the concentration of effluents is monitored with a quadrupole mass spectrometer (SXP 300, VG Instruments) connected between the plasma reactor and the pump. The distance between the lower electrode and the entrance of the mass spectrometer is about 20 cm. Typical operation conditions are as follows: ion energy 5 eV, electron energy 70 eV, emission current 0.5 mA. The emission spectra were collected through a quartz window, looking radially inwards and positioned in the middle of the powered electrode. Light is transmitted via an optical fiber to a 0.32-m JOBIN YVON monochromator (HR 320) capable of working with a resolution of 0.04 nm; the photons are detected by a photomultiplier whose spectral response ranges from 185 to 870 nm. The whole process is monitored by a Spectralink apparatus, which can record, store spectra, and integrate peak areas. It is also possible to follow the evolution of a specific peak intensity versus time. Typical experimental conditions are:

100-μm aperture entrance slit, 700-V photomultiplier voltage for an oxygen plasma, and 600 V for an argon plasma.

Procedures

The experimental process is as follows: After setting up the samples in the chamber, the reactor is pumped out to 10^{-2} torr, and argon is flowed at 100 $cm^3_{(STP)}$/min until the oxygen concentration measured by mass spectrometer drops below 1%. Then the desired gas flow rate, power, and pressure are adjusted and the plasma is started. When the treatment is over, the samples are kept in the reactor chamber for 10 min more under the same gas flow rate. The weight loss is calculated from the weight of the sample before and after treatment. The concentration of the different species formed by surface degradation are followed by mass spectrometer, which can monitor 16 m/e peak values as a function of time. The subsequent treatment of the stored data enables us to plot their evolution versus the operation conditions. Typically, the initial gas composition was 98% argon, 0.2% hydrogen, 0.7% water, 0.9% azote, and 0.2% oxygen for an argon plasma and 97% oxygen, 0.2% hydrogen, 1% water, 1.4% azote, and 0.3% argon for an oxygen plasma. The emission properties of the plasma gas as well as the degradation products were studied under the same conditions.

RESULTS AND DISCUSSION

Time Influence

Degradation

The weight loss increases linearly with time, as shown in Figure 3, whatever the experimental conditions, even for times as long as one hour in the case of an argon plasma. This result agrees with those found in the literature.[25,32,33] But, during the first seconds, the weight loss is too small to be measured, and it is not possible to claim that degradation occurring during this time is proportional to time. The fact that the degradation rate is constant shows that the evacuation of the calories is efficient enough so that the temperature of the sample surface remains practically constant during the treatment. The degradation is higher for OOD than for $C_{36}H_{74}$ in both oxygen and argon plasmas, pointing out the influence of the ester function in OOD. The weight loss is much more important in an oxygen plasma than in an argon plasma.

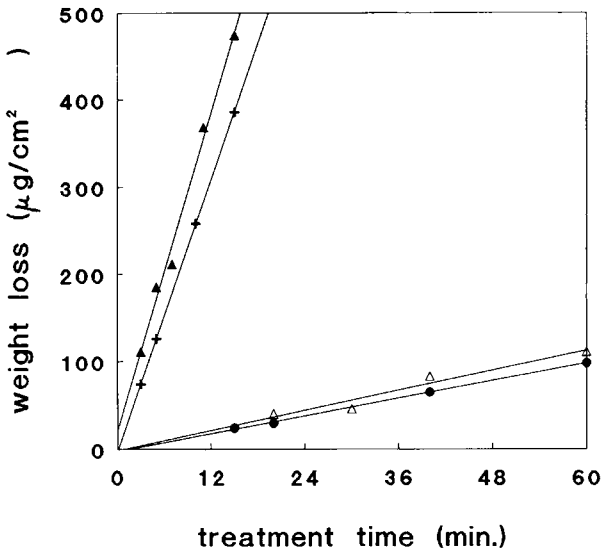

Figure 3 Weight loss of $C_{36}H_{74}$ and OOD films versus time; gas flow rate 40 $cm^3_{(STP)}$/min, pressure 0.3 torr, power 60 W. (▲) OOD O_2, (+) $C_{36}H_{74}$ O_2, (△) OOD Ar, (●) $C_{36}H_{74}$ Ar; calculated error: ± 5%.

Optical Emission Spectroscopy

In emission spectroscopy, the intensities evolution was followed both with and without sample. The study versus time of two characteristic emission lines of Ar and O atoms at 7504 Å and 7772 Å, respectively, shows that the emission appears as soon as the discharge is started and reaches almost instantly a plateau (within 0.4 s). When samples are present in the discharge, these two emission intensities are lower than the corresponding ones in the background, but they are equivalent regardless of the surface nature. In fact, we have checked that the larger the organic film surface, the higher the intensity decrease. This behavior can be due to a modification of the electronic density induced by the presence of a dielectrics on the grounded electrode and/or by the intervention of the fragments coming from the surface with the process of formation of excited species,[34] or/and even by a consumption of the O atoms by the degradation reactions in an oxygen plasma. Conversely, the intensities of the emission lines relevant to the excited degradation products, i.e., CO (2833 Å), CO_2 (2883 Å), and Hα (6563 Å) in an oxygen plasma and CO, Hα, and CH (4315 Å) in an argon plasma increase strongly. The presence of CH fragments in an argon plasma detected in optical emission spectroscopy means that C—C bond breaking exists. Both mass and emission spectroscopies did not detect CO_2 in an argon plasma.

In order to take into account the molecules that could stem from the reactor walls, the intensity differences between the spectra obtained with and without a sample were calculated for lines characteristic of the degradation products. The values obtained are reported in Table I. According to the relative degradation rates, the line intensities of the degradation products are higher for OOD than for $C_{36}H_{74}$ in both oxygen and argon plasmas.

Mass Spectrometry

Mass spectrometry enables us to follow the formation and evolution of neutral molecules resulting from the degradation from the very first seconds. It was found that in an oxygen plasma, H_2O, CO, CO_2, and H_2 (m/e: 18, 28, 44, 2) are the main degradation products, whereas in an argon plasma, only H_2 and CO were monitored. The other stable fragments, if they exist, were in too small quantities to be detected. The intensity differences between the two spectra with and without sample were calculated as before.

It was checked that the pressure fluctuations induced very small changes of H_2, CO, CO_2 and H_2O, negligible as compared to the recorded differences, and that the fragmentation of CO_2 through ionization in the mass spectrometer produces a signal at m/e equal to 28 whose intensity is no more than 10% of that at $m/e = 44$. These values are therefore representative of the molecules stemming from the $C_{36}H_{74}$ or OOD surface.

In an oxygen plasma, the concentrations of CO and CO_2 increase very quickly during the first 20 s and then stabilize, while that of H_2 and H_2O increase slowly for 2 min (Fig. 4, a_1 and a_2). This result shows that oxygen incorporation on the surface is very rapid and leads immediately to the formation of CO and CO_2. In the case of $C_{36}H_{74}$, the intensity of H_2O becomes higher than that of CO while in the case of OOD, CO intensity stays always higher than that of H_2O.

In the case of an argon plasma (Fig. 4, b_1 and b_2), the H_2 concentration reaches a maximum after about 20 s, faster than in an oxygen plasma, and then decreases slightly to a plateau; it is the main degradation product. H_2O traces could be detected only during the first 30 s. No CO_2 coming from the surface was detected even in the case of OOD, indicating that the bond breaking to release CO_2 from the ester is negligible. The peak at 28 is due to CO whose formation is possible since traces of oxygen (less than 1% in all cases) were still present in the argon plasma. The H_2, CO, CO_2, and H_2O mass spectrometry intensities (C), degradation rates (R_D) for $C_{36}H_{74}$ and OOD as well as their ratios are given in Table II. Under those conditions, the concentration ratios for all degradation products are in good agreement with those of the degradation rates. The fact that the H_2 concentration in an argon plasma is about a third that of an oxygen plasma (Table III) and 6 times smaller than the sum of H_2 and H_2O whereas the degradation rate is about 15 times smaller, indicates that H atom abstraction through —C—H bond breaking in an argon plasma is the main degradation process. $—CH_2—CH_2—$ bond breaking will not be responsible for significant weight loss because of the very rapid dismutation reaction of the $—CH_2^{\bullet}$ radicals according to the following reaction scheme[35]:

$$2 \sim CH_2—CH_2^{\bullet} \rightarrow \sim CH=CH_2 + \sim CH_2—CH_3 \quad \sim CH_2—CH_2^{\bullet} + \sim CH_2—CH_2 \sim \rightarrow \sim CH_2—CH^{\bullet} \sim + \sim CH_2—CH_3$$

Table I Emission Intensities of Degradation Products in Oxygen and Argon Plasmas for $C_{36}H_{74}$ and OOD

O_2	$C_{36}H_{74}$	OOD	Ar	$C_{36}H_{74}$	OOD
I_{CO}	1294	2045	I_{CO}	213	191
I_{CO2}	685	1414	I_{CH}	132	181
I_{Ha}	12601	32209	I_{Ha}	1898	2376

Power Influence

Degradation

Keeping the pressure and the gas flow rate constant, the reactions were carried out with increasing power. The degradation rates increase linearly with the applied power (P_w) in both an oxygen and an argon plasma in agreement with those observed for many other polymers,[33,36,37] but extrapolation of these straight lines at $P_w = 0$ do not go through zero. Then, the degradation rates versus power can be expressed by the following equation:

$$R_D = a_D[P_W] + b_D$$

The values of a_D and b_D are given in Table IV. The slopes for $C_{36}H_{74}$ and OOD are equivalent in both an oxygen and an argon plasma indicating that in the range studied, the effect of the ester function is independent of the power applied. It seems that an acceleration exists at lower power, which increases with the degradation rates: OOD > $C_{36}H_{74}$ and O_2

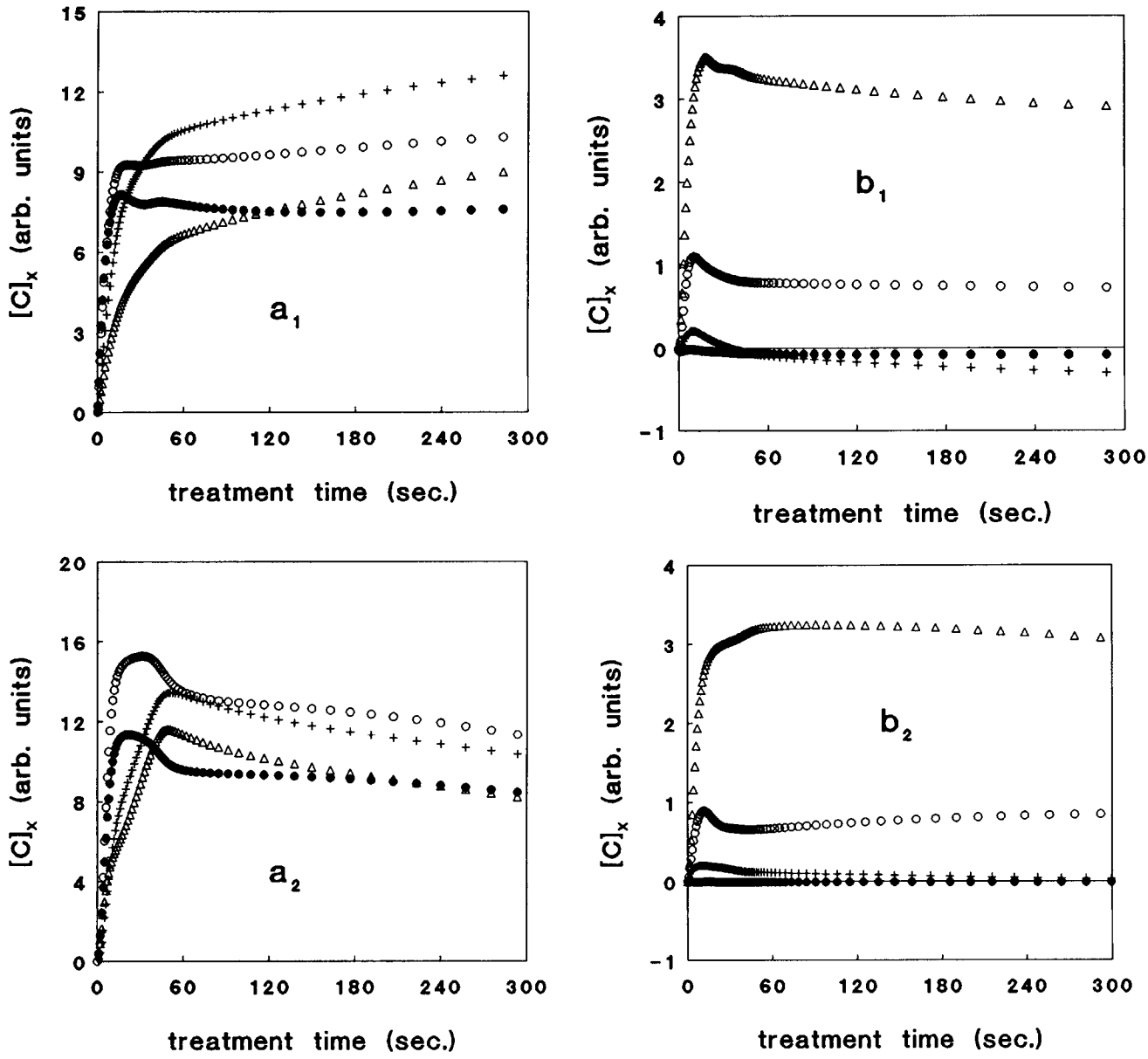

Figure 4 H_2O (+), CO (○), H_2 (△), and CO_2 (●) mass spectrometry concentration versus treatment time for a_1, $C_{36}H_{74}$; a_2, OOD in oxygen plasma and b_1; $C_{36}H_{74}$; b_2; OOD in argon plasma; estimated error: ±10%.

> Ar (see b_D in Table IV). The ratio of the slopes a_D between an oxygen plasma and an argon plasma is 20 for $C_{36}H_{74}$ and 18.5 for OOD, showing that the presence of an ester group reduces the degradation difference between the two types of plasmas. This is confirmed by the subsequent study of the corresponding polymers.

Optical Emission Spectroscopy

The study of optical emission spectroscopy versus power shows that:

1. The emission intensity of atomic O (7772 Å) increases as $P_w^{2.3}$ and that of Ar (7504 Å) as $P_w^{0.42}$. The introduction of a sample does not modify this behavior. When a sample is present, the intensity is always smaller than that of the background; the higher the applied power, the more important the difference between them. But the intensity difference between two samples, $C_{36}H_{74}$ and OOD, is difficult to estimate even at 100 W.

2. In an oxygen plasma [Fig. 5(a)], the emission intensity due to the degradation products (CO, CO_2, and Hα) are higher for OOD than for $C_{36}H_{74}$, in

Table II Degradation Rates (R_D in $\mu g/cm^2 \cdot min$) and Mass Spectrometer Signal Intensities versus Operation Conditions for Hexatriacontane and OOD

	Effluent Peak Intensity				
	H_2	H_2O	CO	CO_2	R_D
O_2 plasma					
$C_{36}H_{74}$	8.7	10.6	9.5	8.1	25.9
OOD	10.1	11.0	11.8	9.3	29.7
Ratio	0.86	0.96	0.8	0.87	0.87
Ar plasma					
$C_{36}H_{74}$	3.1	0	0.8	0	1.66
OOD	3.1	0	0.8	0	1.91
Ratio	1.00	—	1.00	—	0.87

Table IV Slopes of Curves of Degradation Rates and of [CO], [H_2], [CO_2] Concentrations versus Power for $C_{36}H_{74}$ and OOD in an Argon and an Oxygen Plasma

	$C_{36}H_{74}$		OOD	
	O_2	Ar	O_2	Ar
a_D [R_D]	0.27	0.014	0.28	0.015
b_D	10.3	0.64	18.4	1
a_c [CO]	0.1	—	0.2	—
a_I [CO]	30.6		40.5	
a_I [CO_2]	19.8	—	28.2	—
a_c [H_2]	0.3	0.03	0.1	0.01
a_I [Hα]	—	31	—	—
a_I [CH]	—	3.8	—	4
a_c [H_2O]	0.13	—	0.1	—

agreement with the degradation rates. For Hα, this value increases as P_w^b (b = 3.12 for $C_{36}H_{74}$ and b = 2.8 for OOD) whereas that for the CO and CO_2 lines increases linearly with power. The slopes (a_I in Table IV) are also higher for OOD than for $C_{36}H_{74}$.

3. In an argon plasma [Fig. 5(b)], Hα intensity for $C_{36}H_{74}$ increases linearly with power, while for OOD, it reaches a plateau. For both $C_{36}H_{74}$ and OOD, the intensity of the CH line increases linearly with power and that of CO increases slightly before staying constant. The intensity difference of the degradation products between $C_{36}H_{74}$ and OOD is not very significant. Conversely, this confirms that the degradation rates of $C_{36}H_{74}$ and OOD are very close to each other.

Mass Spectrometry

The intensities of the CO, H_2, and H_2O mass spectrometry signals in an oxygen plasma increase linearly with power in accordance with the degradation rates and can also be expressed as

$$[C] = a_C[P_W] + b_C$$

where [C] is the peak intensity of mass spectrometry, which is representative of the fragment concentration in the gas phase. The values of a_c and b_c are presented in Table IV, we can observe that:

1. In an oxygen plasma, the formation of H_2 increases faster than that of CO and H_2O for $C_{36}H_{74}$ [Fig. 6(a)], and its concentration becomes higher than that of OOD from 60 W; in the case of OOD [Fig. 6(b)], it is the formation of CO that exhibits the highest rise, and its concentration is always higher than that relative to $C_{36}H_{74}$.

2. In an argon plasma, the evolution of CO and H_2 concentrations versus power is comparable to that observed in photoemission for CO and Hα lines (Fig. 7).

In the case of an oxygen plasma, CO_2 does not increase linearly with power; its concentration becomes stable at 60 W for both $C_{36}H_{74}$ and OOD and is higher for OOD.

When the power is raised, both the electron energy and its density increase, and the reactive particles become more energetic. The abstraction of H atoms and the subsequent scission of surface chains are enhanced, promoting degradation. From the above discussions it can be concluded that:

1. The degradation rate is higher for OOD than for $C_{36}H_{74}$, but an increase of power does not modify the influence of the ester group on the degradation behavior.

2. The formation of H_2 increases the strongest with increasing power for $C_{36}H_{74}$ whereas for OOD, CO exhibits the highest rise, in an oxygen plasma.

3. Both the concentration and the emission intensities of the degradation products agree with the

Table III Ratio of H_2 and CO Mass Spectrometry Intensities and of Degradation Rates in Oxygen and Argon Plasmas[a]

	X(H_2)	X(CO)	X(R_D)
$C_{36}H_{74}$	2.8	11.8	15.6
OOD	3.2	14.7	15.5

[a] X(H_2) is the ratio of the H_2 peak intensity in an oxygen plasma over that in an argon plasma, X(CO) is the ratio of the CO peak intensity in an oxygen plasma over that in an argon plasma, and X(R_D) is the ratio of the degradation rate in an oxygen plasma over that in an argon plasma.

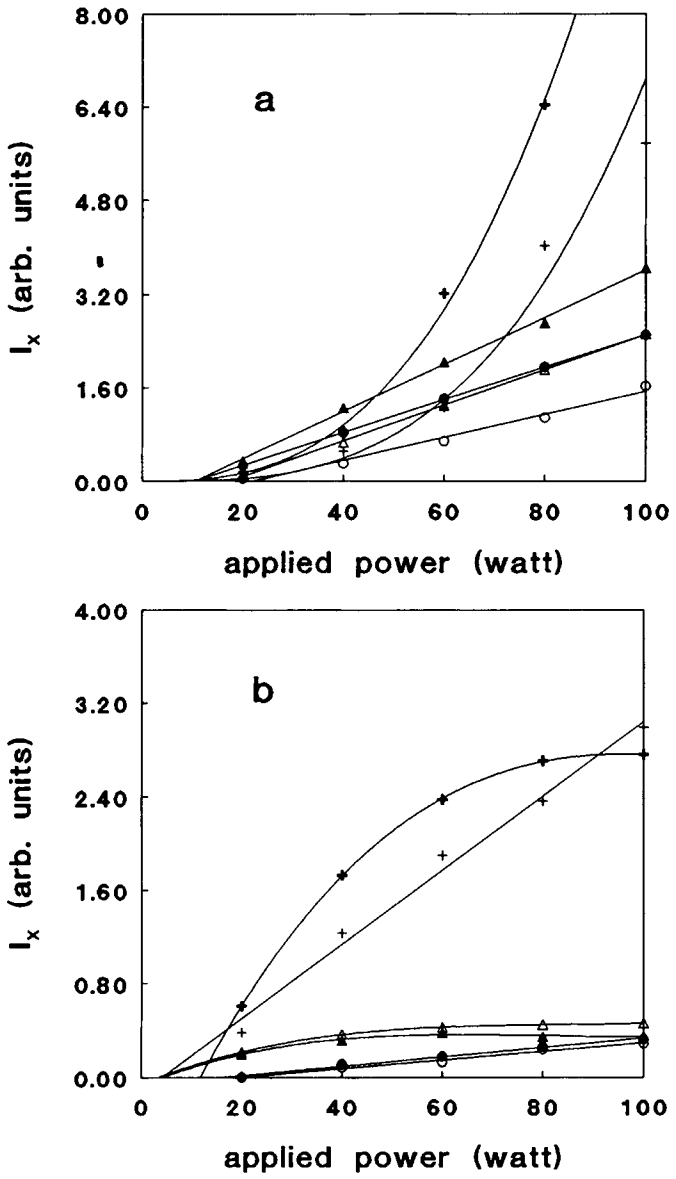

Figure 5 Evolution of emission intensities of the prominent species versus applied power: (a) in oxygen plasma (+) Hα, (▲) CO, and (●) CO_2 and (b) in argon plasma (+) Hα, (▲) CO, and (●) CH for OOD and for $C_{36}H_{74}$ (a) in oxygen plasma (+) Hα, (△) CO, and (○) CO_2 and (b) (+) Hα, (△) CO, and (○) CH in argon plasma (60 W, 40 $cm^3_{(STP)}$/min, 0.3 torr); estimated error: ±15%.

degradation rates; CO is the most representative of the weight loss in the case of an oxygen plasma.

4. The emission intensity of atomic O and Ar excited species varies as P_w^a while the degradation rate increase is linear. But, the emission intensity cannot be directly related to the concentration of excited species, so it is not surprising that the degradation rates did not vary like emission intensities. In fact, several phenomena should be taken into account to correlate the degradation rate with the power such as the electron and the ion bombardment and UV irradiation of the surface.

Formation of the Degradation Products

Discussion of the Mechanism

In an argon plasma, the argon excited species cannot chemically react with the surface and the formation of radicals is attributed to the ion bombardement.

In an oxygen plasma, beside the ion bombardement, atomic oxygen[45] seems to be the species responsible for the initiation of the reaction according to:

$$RH + O \rightarrow R^{\bullet} + OH^{\bullet}$$

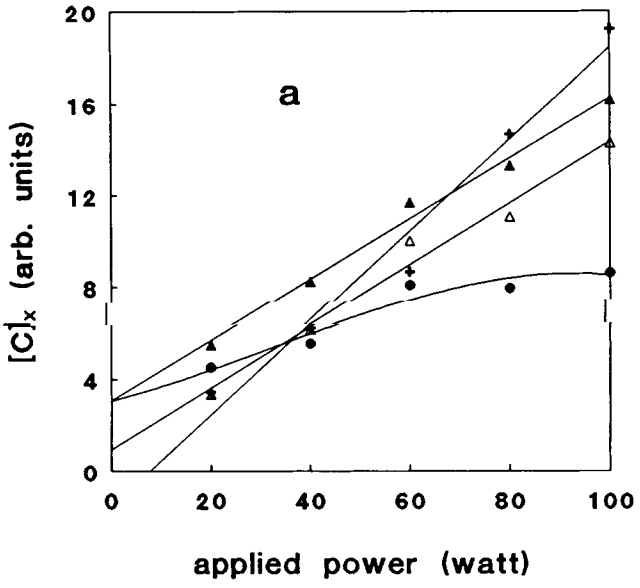

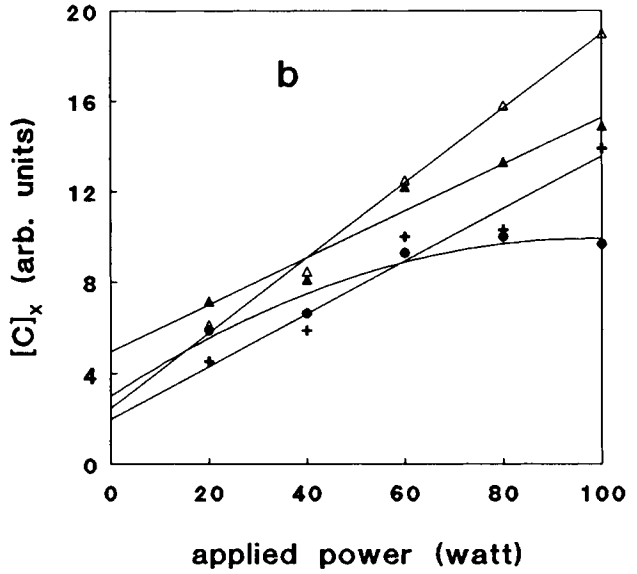

Figure 6 Concentration of degradation product versus power in oxygen plasma. (a) $C_{36}H_{74}$ (b) OOD. (+) H_2, (▲) H_2O, (△) CO, (●) CO_2; estimated error: ±10%.

followed by

$$RH + OH^{\bullet} \rightarrow R^{\bullet} + H_2O$$

The rate constants of $OH^{\bullet}$ and $H^{\bullet}$ radicals and atomic oxygen toward butane[38] (at 25°C) have been reported as follows:

$$K_{OH} = 2.7 \times 10^{-12} \qquad K_{O(3P)} = 2.2 \times 10^{-14}$$

and $K_H = 2.5 \times 10^{-16}$ cm^3 molecule^{-1} s^{-1}

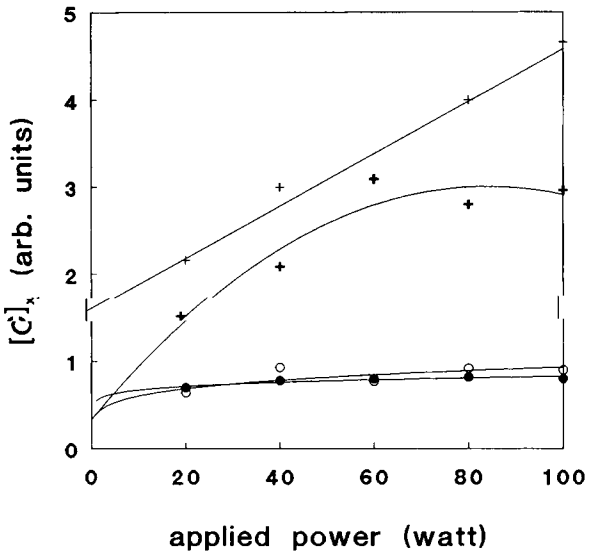

Figure 7 Concentration of degradation product versus power in argon plasma. (+) H_2, (●) CO For OOD and (+) H_2, (○) CO for $C_{36}H_{74}$; estimated error: ±10%.

$OH^{\bullet}$ are very reactive and therefore their concentration will stay low as compared to that of atomic O.

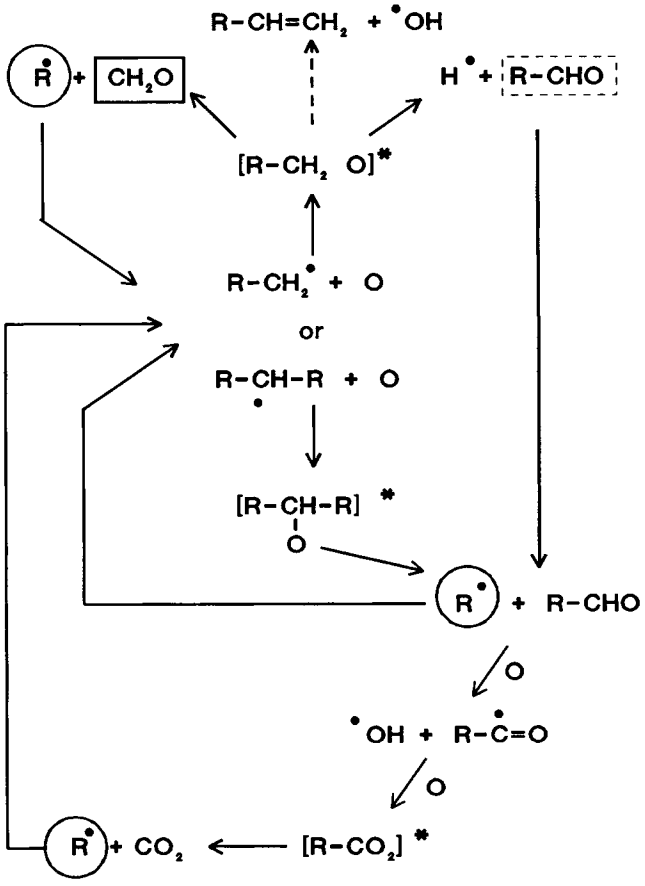

Figure 8 Atomic oxygen reaction with alkyl radicals.

The primary or secondary radicals formed can react with molecular oxygen or atomic oxygen. With molecular oxygen, the formation of peroxy radicals and hydroperoxydes according to the following mechanism has been proposed[39]:

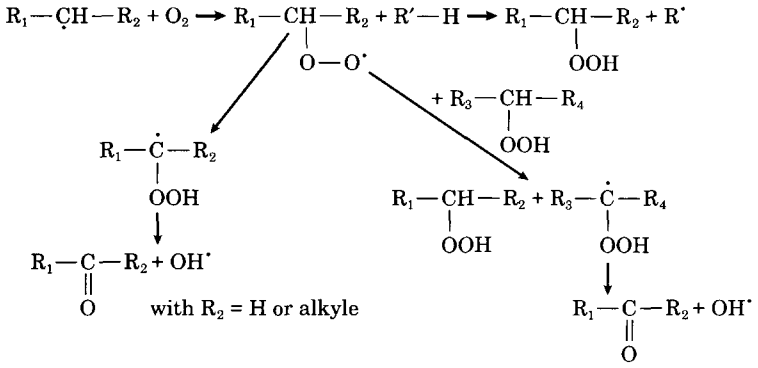

The peroxy radicals, hydroperoxydes, aldehydes, and ketones are able to react with one another to produce ketones, aldehydes, alcohols, acids, and vinyl groups according to the mechanism of polyethylene photooxydation.[40]

Atomic oxygen attacks primary or secondary radicals to give the reactions as reported in Figure 8 according to Huie et al.,[41] inducing the propagation of the degradation.

The radicals produced will be attacked again by atomic oxygen, inducing complete degradation of the chains and formation of formaldehyde, which can also react with atomic oxygen according to the following mechanism[41]:

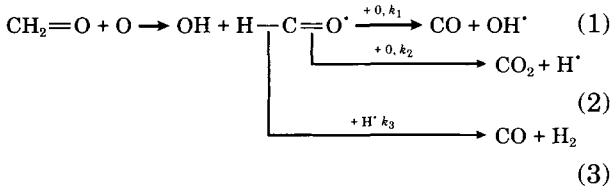

(1)

(2)

(3)

with $k_3/(k_1 + k_2) \simeq 3 \pm 2$ and $k_1/k_1 \simeq 1.2$

The reaction of alkyl radicals with atomic oxygen will result in the formation of CO, CO_2, OH·, and H· radicals and vinylic groups on the surface.

OH· radicals are able to react according to various reactions:

$$OH^{\cdot} + RH \xrightarrow{k_4} R^{\cdot} + H_2O \quad (4)$$

$$OH^{\cdot} + CO \xrightarrow{k_5} CO_2 + H^{\cdot} \quad (5)$$

$$OH^{\cdot} + H_2 \xrightarrow{k_6} \boxed{H_2O} + H^{\cdot} \quad (6)$$

$$OH^{\cdot} + OH^{\cdot} \xrightarrow{k_7} \boxed{H_2O} + O \quad (7)$$

$$OH^{\cdot} + H^{\cdot} \xrightarrow{k_8} \boxed{H_2O} \quad (8)$$

$$OH^{\cdot} + O \xrightarrow{k_9} O_2 + H^{\cdot} \quad (9)$$

According to Avramenko,[42] $k_4 > k_5 > k_6$. Reactions (6), (7), and (8) are unlikely at least during the first seconds of treatment.

It appears that H_2O is formed essentially in reactions involving OH·. This explains why its concentration increases more slowly with time than that of CO and CO_2 formed directly via atomic oxygen reactions.

The concentration of CO_2 in the gas phase is the result of the competition between its formation [Eq. (5) and (10)] and its decomposition [Eq. (11) and (12)]:

$$CO + OH^{\cdot} \rightarrow CO_2 + H^{\cdot} \quad (5)$$

$$CO + O \rightarrow CO_2 \quad (10)$$

$$CO_2 \rightarrow CO + \tfrac{1}{2}O_2 \quad (11)$$

$$CO_2 + e \rightarrow CO + O \qquad E > 10\ \text{eV/mol}^{43} \quad (12)$$

The formation of CO_2 is directly dependent of that of CO, and this fact is confirmed by its evolution with time, which is parallel to that of CO. When power increases, CO_2 reaches a plateau. This can be explained by Eq. (12), which is favored by the increase of the electron energy. Moreover, Tanaka and Miyoshi[44] showed that the decomposition of CO_2 into CO increases with power injected in the discharge.

H· radicals are formed via reactions (2), (5), (6), and (9), and the following reactions give an account of the formation of H· radicals and hydrogen:

$$H{-}C{=}O^{\cdot} + H^{\cdot} \rightarrow H_2 + CO \quad (3)$$

$$RH + H^{\cdot} \rightarrow H_2 + R^{\cdot} \quad (13)$$

$$2H^{\cdot} + S \rightarrow H_2 \quad (S: \text{third body}) \quad (14)$$

H° is less reactive than OH° radicals and atomic oxygen, and therefore the formation of H_2 is in competition with other reactions.

In an argon plasma, reactions (13) and (14) explain the formation of H_2. This is the main gaseous degradation product. Its concentration reaches a plateau much more rapidly than in the case of an oxygen plasma because there is no consumption of H° radicals by the other reactions reported above.

From the mechanism proposed, which agrees well with the evolution of degradation products versus time, it appears that, in an oxygen plasma:

1. The degradation should result directly from the action of atomic oxygen while both atomic oxygen and molecular oxygen would take part in the functionalization.
2. Ion bombardment, O atoms and OH° radicals are responsible for the initiation of the degradation reactions.
3. Atomic oxygen is responsible for the propagation of degradation and CO and CO_2 should be mainly formed through the attack of formaldehyde.
4. Water formation, which results from the action of OH° radicals, increases obviously more slowly than that of CO and CO_2.
5. A steady state between the different compounds formed is established after about 2 min. A power increase shifts this steady state.

The mechanism proposed above cannot explain the higher degradation of OOD compared to that of $C_{36}H_{74}$. In terms of bond energy, the probability of breaking is the same for $C_{36}H_{74}$ and OOD (see bond energy below[45]).

$$CH_3-\underset{\displaystyle H}{\underset{|}{CH}}\,(CH_2)_n-CH_3:\ 98\ \text{Kcal/mol}$$

$$CH_3-CH_2\!\mid\!(CH_2)_n-CH_3:\ 82\ \text{Kcal/mol}$$

$$CH_3-CH_2-CO_2\!\mid\!(CH_2)_n-CH_3:\ 83\ \text{Kcal/mol}$$

$$CH_3-CH_2-\underset{\displaystyle O}{\underset{\|}{C}}\!\mid\!O-(CH_2)_n-CH_3:\ 94\ \text{Kcal/mol}$$

But, in the case of OOD, the breaking of $RC(O)-OR'$ or RCO_2-R' leads to radicals that are more stable than those formed in C—C bond breaking because of their stabilization by resonance:

$$[R-C\overset{\displaystyle O}{=}]^{\bullet} \quad \text{and} \quad [R-\underset{\displaystyle O}{\underset{|}{C}}=O]^{\bullet}$$

Therefore, chain breaking will be favored in the case of OOD and the degradation initiation rate will increase.

CONCLUSION

In this work we have studied the influence of plasma parameters (treatment time, power) on the behavior of two model molecules $C_{36}H_{74}$ and OOD in oxygen or argon plasmas. The degradation rates, the formation and evolution of the degradation products, as well as their optical emission behavior have been investigated. The following conclusions can be drawn:

1. Degradation is higher in an oxygen plasma than in an argon plasma; the presence of only one ester functional group in OOD clearly increased the rates of weight loss.
2. CO, H_2O, CO_2, and H_2 are the main degradation products in an oxygen-rich plasma whereas H_2 is the most important in an argon-rich plasma.
3. The intensity of the degradation products detected by mass spectrometry is in good agreement with rates of weight loss measurement.
4. The degradation products are the same for both model molecules, but when the power increases, the formation of H_2 and H_2O is favored in the case of $C_{36}H_{74}$, while in the case of OOD, it is CO that is enhanced.
5. A mechanism has been proposed to explain the relative concentrations of the degradation products in the gas phase.

REFERENCES

1. D. K. Owens, *J. Appl. Polym. Sci.*, **19,** 265 (1975).
2. A. R. Blythe, D. Briggs, C. R. Kendahl, D. G. Rance, and V. J. I. Zichy, *Polymer,* **19,** 273 (1978).
3. T. E. Nowlin and D. F. Smith, *J. Appl. Polym. Sci.,* **25,** 1619 (1980).
4. M. Neush and J. Kieser, *Vacuum,* **34,** 959 (1984).
5. J. C. Boeda, M. De Mendez, G. Legeay, and J. C. Brosse, *Revue générale d'électricité,* **5,** 15 (1987).
6. J. Amouroux, F. Arefi, P. Spartacus, S. Mournet, and M. Goldmann, *Polym. Mater. Sci. Eng.,* **56,** 332 (1987).
7. H. Gleich, R. M. Criens, H. G. Mosle, and U. Leute, *Int. J. Adhesion Adhesives,* **9,** 88 (1989).
8. D. T. Clark and A. Dilks, *J. Polym. Sci. Polym. Lett. Ed.,* **18,** 541 (1979).

9. R. G. Nuzzo and G. Smolinsky, *Macromolecules,* **17,** 1013 (1984).
10. J. M. Pochan, L. J. Gerenser, and J. F. Elmann, *Polymer,* **27,** 1058 (1986).
11. T. J. Hook, J. A. Gardella, and S. Lawrence, *J. Mater. Res.,* **2,** 117 (1987).
12. M. Strobel, S. Corn, C. S. Lyons, and G. A. Korba, *J. Polym. Sci. Polym. Chem.,* **25,** 1295 (1987).
13. J. M. Loh, M. Klausner, R. F. Baddour, and R. E. Cohen, *Polym. Eng. Sci.,* **207,** 861 (1987).
14. T. G. Vargo, J. A. Gardella, and S. Lawrence, *J. Mater. Res.,* **27,** 1267 (1989).
15. R. Foerch, N. S. Mcintyre, and R. N. S. Sodhi, *J. of Appl. Polym. Sci.,* **40,** 1903 (1990).
16. N. Inagaki, S. Tasaka, and H. Miyazaki, *J. Appl. Polym. Sci.,* **38,** 1829 (1989).
17. F. Poncin-Epaillard, B. Chevet, and J. C. Brosse, *Eur. Polym. J.,* **26,** 333 (1990).
18. N. Suzuki, A. Kishida, H. Iwata, and Y. Ikada, *Macromolecules,* **19,** 1804 (1986).
19. H. S. Munro and C. Till, *J. Polym. Chem. Polym. Chem.,* **24,** 279 (1986).
20. M. Hudis, *J. Appl. Polym. Sci.,* **16,** 2397 (1972).
21. D. T. Clark and A. Dilks, *J. Polym. Sci.,* **15,** 2321 (1977).
22. A. H. Zahran, E. Nofal, M. Z. Elsabee, and M. A El-Azmirly, *J. Appl. Polym. Sci.,* **24,** 1723 (1979).
23. V. Iriyama and H. Yasuda, *Polymeric Mater. Sci. Eng.,* **56,** 327 (1987).
24. S. J. Moss, A. M. Jolly, and B. J. Tighe, *Plasma Chem. Plasma Process.,* **6,** 401 (1986).
25. M. Kogoma and G. Turban, *Plasma Chem. Process.,* **6,** 349 (1986).
26. S. R. Cain, F. D. Egitto, and F. Emmi, *J. Vac. Sci. Technol.,* **A5,** 1578 (1987).
27. N. R. Lerner and T. Wydeven, *J. Appl. Polym. Sci.,* **35,** 1909 (1988).
28. M. K. Shi, Y. Holl, and F. Clouet, *Bull. Soc. Fr. Phys. Suppl.,* **73,** 25 (1989).
29. M. K. Shi, Y. Holl, and F. Clouet, *Makrom. Chem., Rapid Commun.,* **12,** 277 (1991).
30. R. Boistelle, B. Simon, and G. Pepe, *Acta Cryst.,* **B32,** 1240 (1976).
31. F. Zemlin and D. L. Dorset, *Ultramicroscopy,* **21,** 263 (1987).
32. R. H. Hansen, J. V. Pascale, T. De Benedictis, and P. M. Renzepis, *J. Polym. Sci. Part A,* **3,** 2205 (1965).
33. H. Yasuda, C. E. Lamaze, and K. Sakaoku, *J. Appl. Polym. Sci.,* **17,** 137 (1973).
34. F. Kaufmann and J. R. Kelso, *J. Chem. Phys.,* **32,** 301 (1960).
35. J. F. Rabek and B. Ranby, *J. Polym. Sci. A1,* **12,** 273 (1974).
36. T. Yasuda, M. Gaziicki, and H. Yasuda, *J. Appl. Polym. Sci. Appl. Polym. Symp.,* **38,** 201 (1984).
37. S. Dzioba, G. Este, and H. M. Naguib, *J. Electrochem. Soc.,* **129,** 2537 (1982).
38. R. Atkinson, K. R. Darnall, A. C. Lloyd, A. M. Winer, and J. N. Pitts, *Advanc. Photochem.,* **11,** 375 (1979).
39. J. Petruj and J. Marchall, *Radiat. Phys. Chem.,* **16,** 27 (1980).
40. F. Gugumus, *Die Angew. Makromol. Chemie,* **182,** 111 (1990).
41. R. E. Huie and J. T. Herron, *Prog. Reactions Kinetics,* **1,** 1 (1975).
42. L. I. Avramenko and R. V. Kolesnikova, *Advances Photochem.* **2,** 25 (1969).
43. A. V. Eletskii and B. M. Smirnov, *Pure Appl. Chem.,* **57,** 1235 (1985).
44. K. Tanaka and H. Miyoshi, *9th Int. Symp. on Plasma Chem., Sym. Proc.,* **II,** 1098 (1989).
45. B. Ranby and J. F. Rabek, in *Photodegradation Photooxydation and Photostabilization of Polymers,* Wiley, New York, 1975, p. 46.

Received July 19, 1991
Accepted February 20, 1992